



Full Length Article

Utilizing *Cinnamomum verum* extract for green synthesis of silver nanoparticles: Exploring optical properties, morphology, and potential applications

Meznah M. Alanazi

Department of Physics, College of Science, Princess Nourah bint Abdulrahman University, P.O. Box 84428, Riyadh 11671, Saudi Arabia

ARTICLE INFO

Keywords:

Green synthesis
Cinnamomum verum
 AgNPs
 Optical properties
 MTT assay

ABSTRACT

One of the most widely used medicinal herbs, cinnamon verum, has numerous pharmacological applications in traditional medicine. In this work, an aqueous extract of *Cinnamomum verum* (Cv) was used to produce silver nanoparticles (AgNPs). Numerous methods were used to study the Cv-AgNPs, including transmission electron microscopy(TEM), dynamic light scattering(DLS), ultraviolet–visible spectrophotometry(UV–vis), energy-dispersive spectroscopy (EDS), X-ray diffraction(XRD), and Fourier-transform infrared spectroscopy (FT-IR). The face-centered cubic(FCC) crystal structure of the Cv-AgNPs, with an average crystallite size of 19.25 nm, has been revealed by XRD pattern analysis. The MTT assay was utilized to evaluate the anti-tumor and cytotoxic effects of Cv-AgNPs on MCF-7 and HeLa cell lines. Moreover, the anticancer activity of Cv-AgNPs was demonstrated using human cervical cancer cells(HeLa) and the breast cancer cell line(MCF-7). The results showed that Cv-AgNPs demonstrate in vitro cell viability of 9 % and 6 % for HeLa and MCF-7 cell line, respectively, based on 500 μ l of Cv-AgNPs consumed for 24 h. This revealed the Cv-AgNPs' potency as an anticancer agent. Taking everything into account, this work proposes an environmentally friendly way to synthesize Cv-Ag NPs, which may find use in bio-nanomedicine.

1. Introduction

With applications in numerous disciplines such as medicine, biology, pharmaceutical sciences, material science and chemistry nanotechnology has become a cutting-edge technology (Pradhan et al., 2024). Many chemical and physical techniques, including chemical reduction, thermal decomposition, Various chemical and physical methods, such as chemical reduction and thermal decomposition, are available for nanoparticle synthesis, but they often involve costly and hazardous chemicals. In recent years, biological approaches have emerged as the preferred method due to their safety, affordability, and eco-friendliness. While many metals can be used for nanoparticle synthesis, silver is most commonly employed because of its unique properties, including enhanced stability, superior electrical and thermal conductivities, and promising bioactivities like larvicidal and wound-healing effects (Das and Ashraf, 2024).

Nano-biotechnology, a discipline specializing in producing minute particles, holds significant potential in medical and health sectors. These submicron particles offer unique structural, biological, and optical properties, making them valuable for various applications such as drug

delivery, biosensors, and regulating cell proliferation. Metal-based nanoparticles, including titanium, magnesium, iron, zinc, and silver, exhibit diverse structures and functions. Silver nanoparticles, in particular, play crucial roles in cellular processes, acting as analytical and diagnostic tools for identifying bodily ailments and modulating cellular activities (Easmin and Bhattacharyya, 2024; Vikulova and Karakovskaya, 2023).

Silver (Ag) is esteemed as a precious noble metal (Dhaka and Mali, 2023) due to its versatile applications in biomedical fields, biosensors, and cosmetic fibers. Green synthesis methods for silver nanoparticles offer several advantages over traditional physical and chemical approaches, including reduced pollution, lower environmental impact, cost-effectiveness, and fewer required instruments. Utilizing microorganisms in green synthesis is particularly beneficial due to their accessibility, ease of cultivation, and non-toxic nature. Alternatively, plant-based extracts provide a diverse array of metabolites, such as proteins and enzymes, which act as organic reducing and stabilizing agents, making them valuable resources for nanoparticle synthesis (Sari and Suchi, 2023).

Cinnamomum verum stick extract has been used for the production of

E-mail address: mmalenazy@pnu.edu.sa.

<https://doi.org/10.1016/j.jksus.2024.103312>

Received 12 March 2024; Received in revised form 30 May 2024; Accepted 15 June 2024

Available online 17 June 2024

1018-3647/© 2024 The Author. Published by Elsevier B.V. on behalf of King Saud University. This is an open access article under the CC BY-NC-ND license (<http://creativecommons.org/licenses/by-nc-nd/4.0/>).

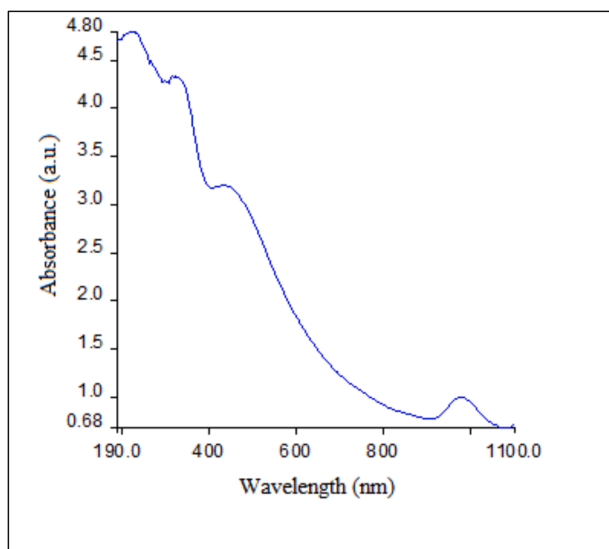


Fig. 1. UV-vis spectrum of synthesized Cv-AgNPs.

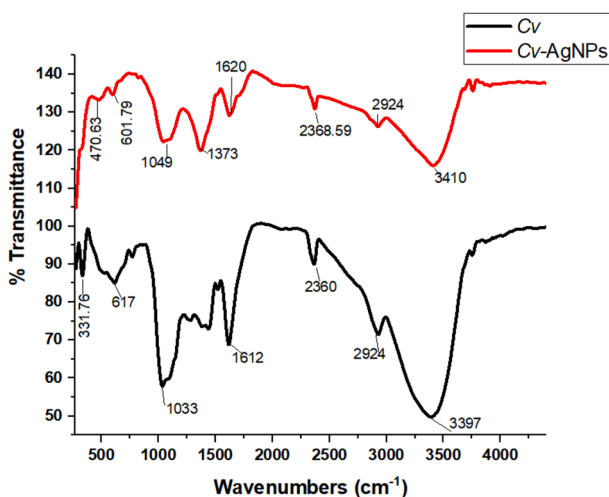


Fig. 2. FTIR spectrum analysis of Cv extract and Cv-AgNPs.

metal oxide and other metallic nanoparticles, including Cu, Au, Ag, and Se. *Cinnamomum* contains cinnamic acid, a capping agent. However, research has proven that polyols, such as terpenoids, flavones, and polysaccharides, are responsible for the bio-reduction of Ag^+ and AuCl_4^- ions (Demirtas and Erenler, 2013; Saqib et al., 2022). Based on additional research, the *C. verum* extract has over 80 aromatic components, including eugenol, saponins, terpenes, alkaloids, flavonol, tannin, cinnamyl aldehyde, corvalol, and glycerol (Ansari et al., 2020).

We are looking into growing this process by finding the biosynthetic route of producing AgNPs from *Cinnamomum verum* extract. The idea is to synthesize and reduce the substance in a way that is both economically and ecologically expedient. We are focusing on stabilizing and reducing the substance in question. By employing UV spectroscopy and Fourier transform infrared spectroscopy, we undertake the process of analyzing the synthesized AgNPs. SEM and EDS, respectively, have been used to confirm the presence of Ag at the nanoscale. In addition, transmission electron microscopy is used to determine the size and shape of the particle gets analyzed. In parallel, we are examining the cytotoxic potential of the AgNPs.

2. Material and methods

2.1. Preparation of plant extract

Sticks of *Cinnamomum verum*(Cv), purchased from a local market in Riyadh, Saudi Arabia. In order to make the Cv extract, the Cv sticks were crushed and ground into a powder. Then, precisely 10 g of the powder was mixed with 100 mL of boiling distilled water, let to soak for a night, and finally filtered.

2.2. Synthesis of Cv-AgNPs

The filtrated solution was centrifuged at 1000 rpm for 5 min at room temperature to obtain a pure aqueous extract of Cv. To synthesis Cv-AgNPs, 50 mL of distilled water was used to dissolve silver nitrate (AgNO_3), then following by stirring the aqueous solution of AgNO_3 at 1000 rpm and 30°C . Then, 5 mL of prepared Cv extract with $\text{pH} = 6$ was added to 1 mmol/mL AgNO_3 aqueous solution. Cv-AgNPs were formed due to the reduction of Ag^+ ions to Ag^0 . The sol is observed when the color turns brown, which was observed due to the surface plasmon resonance in the UV-visible spectrum known to Cv-AgNPs.

2.3. Characterization of green-synthesized NPs

In order to characterize the green-synthesized Cv-AgNPs, a UV-visible spectrometer called Lambda 25 (made by PerkinElmer in the United Kingdom) was utilized. Transmission electron microscopy (TEM, JEOL JEM-1011, Tokyo, Japan) revealed dimensions and morphology. Furthermore, the chemical elements of the synthesized sample were analyzed using energy-dispersive X-ray spectroscopy (EDS) within a scanning electron microscope (SEM, Oxford Instruments INCAx-act (Oxfordshire, UK)). Using the Malvern Zetasizer Nano Advance (ZSU3305), a Dynamic Light Scattering (DLS) investigation was conducted to ascertain the size distribution profile of Cv-AgNPs in suspension. With a Perkin-Elmer 100 spectrophotometer, Fourier transform infrared (FTIR) spectra in the $400\text{--}4000\text{ cm}^{-1}$ range were captured. Using a Bruker D8 ADVANCE X-ray diffractometer (Bruker, Billerica, MA, USA), the crystalline structures of the particles were examined.

2.4. Evaluation of cytotoxic effects

The cytotoxicity test on human carcinoma cell lines, including MCF-7 and HeLa strains from breast and cervical carcinoma, respectively, utilized the MTT assay. Cells were cultured under standard conditions to maintain functionality, then exposed to various doses of Cv-AgNPs in a 96-well plate layout. Crystal violet dye assessed cell viability post-incubation, followed by absorbance measurements. The experiment, conducted in triplicates for accuracy, compared results with control cells to determine cytotoxicity. Dose-response curves were analyzed using GraphPad Prism software to estimate the IC_{50} , representing the concentration at which 50 % of intact cells were adversely affected (Rizki et al., 2023).

3. Results and discussion

Green chemistry has been used to synthesize, characterize, and use Cv-AgNPs by reducing AgNO_3 solution using fruit extract of Cv extract. Upon exposure of the extract to an aqueous solution of Ag^+ ions (AgNO_3), the reaction mixture's colour changed from yellowish brown to dark brown. The excitation of surface plasmon vibrations or resonance in the Cv-AgNPs appeared to be the cause of the change in appearance (Awad et al., 2019; Khan et al., 2023). According to Zia et al., the concentration of Ag ions showed that biomolecules attached to create NPs and eventually changed colour. AgNPs are said to give the solution a dark reddish to dark brown colour (Gecer, 2021). In a related investigation, after mixing Cv extract with silver nitrate solution, a

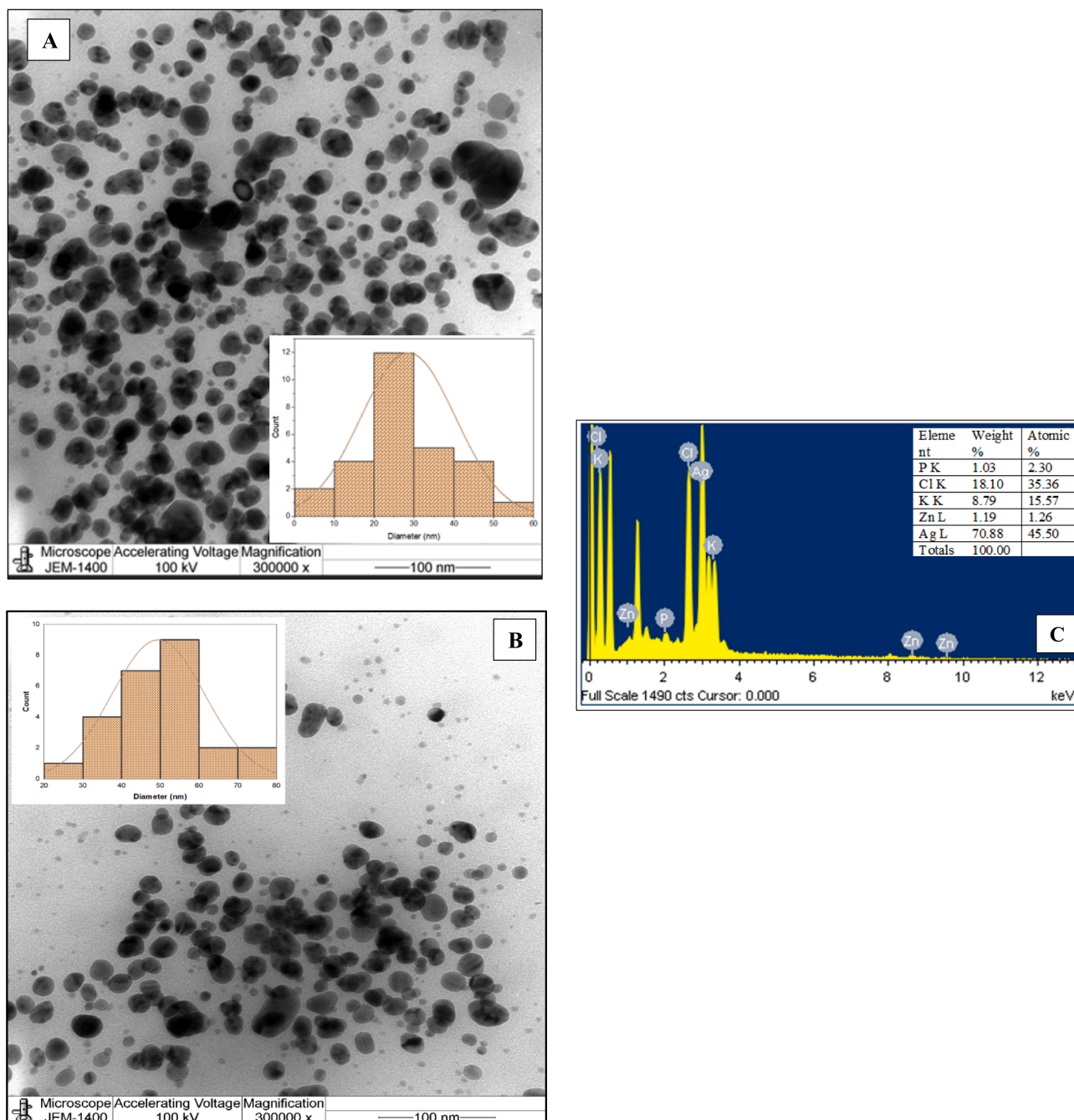


Fig. 3. (A and B) TEM image of synthesized Cv-AgNPs, (C) distribution of elements analysis from Cv-AgNPs by EDS.

colour shift was observed, shifting from light yellow to brown.

The optical characteristics and production of AgNPs utilizing the Cv water extract were determined using the UV-visible spectrum. The synthesized AgNPs' absorbance maxima were found to be 443 nm (Fig. 1). The literature states that the silver nanoparticle Surface Plasmon Resonance (SPR) peak is located between 410 and 455 nm (Zia et al., 2017). The formation of spherical-shaped silver nanoparticles is indicated by the range of absorption bands detected in the 410–455 nm windows, as demonstrated by the strong dependence of Plasmon resonance on nanoparticle size, shape, and dielectric properties (Erenler and Geçer, 2021). As a result, the creation of roughly spherical nanoparticles can be linked to the UV-visible absorbance peak of the synthesized AgNPs at 443 nm. The presence of organic compounds from Cv extract is indicated by additional peaks observed in the UV spectrum of synthesized Cv-AgNPs, specifically around 281 nm and 220 nm

(Maruthamuthu and Ramanathan, 2016). More absorption peaks in the UV spectrum could result from these organic molecules adhering to the AgNPs' surface. Moreover, incomplete reactions or unintended reactions that happen during synthesis could cause these. Moreover, the extra peaks can be indicative of other silver nanoparticle plasmonic modes or surface plasmon resonance. Variations in the size, shape, or aggregation state of nanoparticles may be the cause of these (Sharma et al., 2020; Mani et al., 2021; Amirjani and Firouzi, 2020).

To identify the functional groups of phytochemicals and biomolecules in the plant extract responsible for the stabilization and capping of AgNPs, FTIR analysis was conducted (Fig. 2). FT-IR spectroscopic analysis shows that the carbonyl group of the amino acid residues and protein peptide possesses the strong characteristic of metal binding. Hence, proteins can form a monolayer around metal nanoparticles to mitigate agglomeration into larger assemblages and stabilizing them in

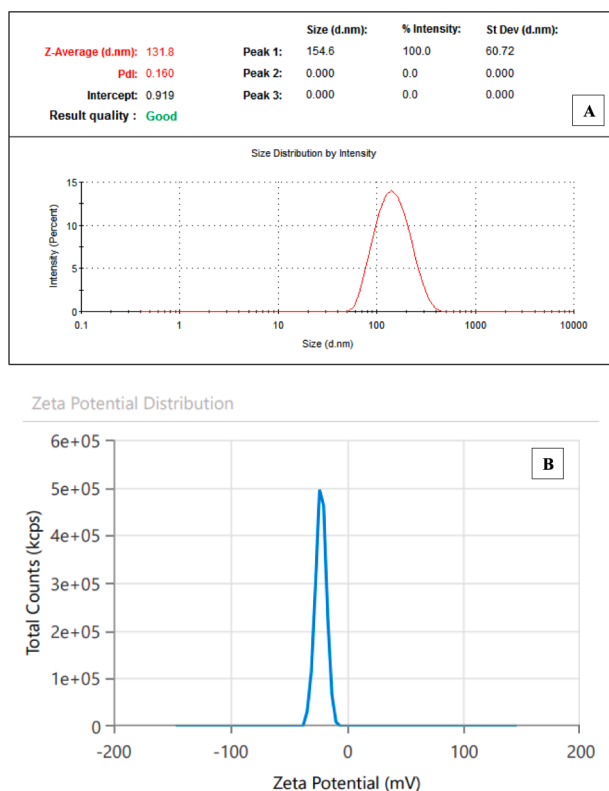


Fig. 4. (A)DLS and (B)zeta potential technique analysis of Cv-AgNPs.

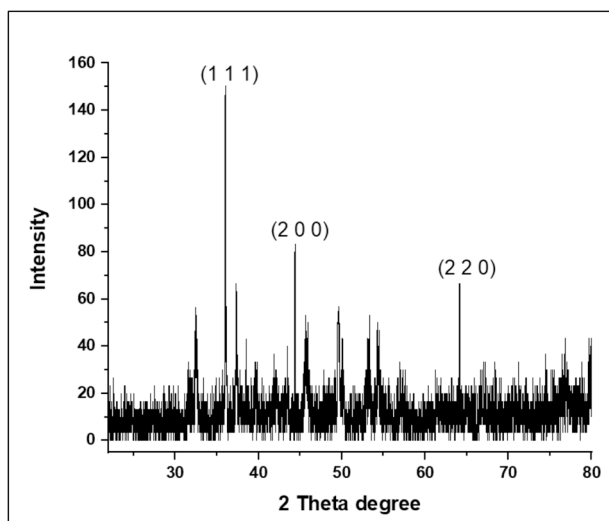


Fig. 5. XRD analysis for Cv-AgNPs.

the solution. Consequently, this experimental data predicts that biomolecules played a role in AgNPs production and aqueous medium stabilization. Two nanoparticles carbonyl groups are bound to proteins through a cysteine group or free amine. The peptides and amino acid residues on the surface of the silver nanoparticles act as capping agents since they can strongly bind to silver ions (Ramirez-Perez et al., 2022). The spectra's bands at 3410 cm^{-1} correspond to the O-H stretching vibration, which shows that phenol and alcohol are present. It was observed that the occurrence of bands at 2368 and 2924 cm^{-1} region are resulting from aromatic compound C-H stretching. The presence of proteins is shown by the band in the spectrum at 1620 cm^{-1} , which corresponds to C-N and C-C stretching. Alkyl halides are known to

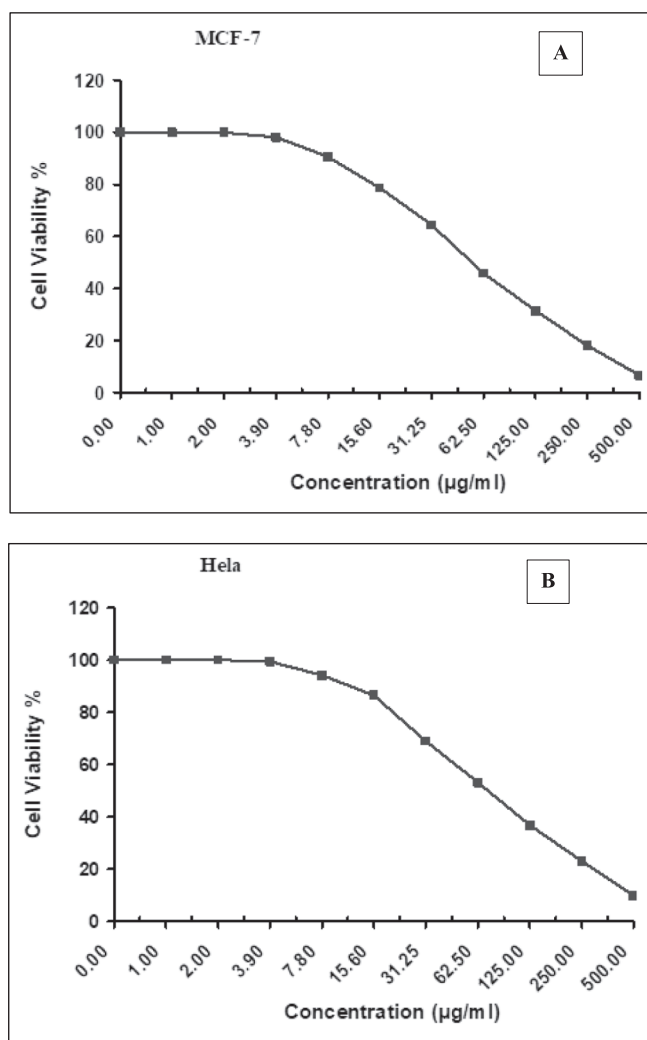


Fig. 6. Assessing the cytotoxic effects on (A) MCF7 and (B) HeLa cell lines after 24 h of exposure to various concentrations of Cv-AgNPs using the MTT assay.

exhibit C-Br stretching, which may be the cause of the band at the $500\text{--}400\text{ cm}^{-1}$ area. The FTIR spectroscopic analysis suggests that the interaction of the proteins in the Cv extract with Ag^+ ions or nanoparticles alters their structure.

Analysis using Transmission Electron Microscopy (TEM) The TEM image in Fig. 3(A and B) revealed more light on size and shape of the synthesized nanoparticles. The image clearly illustrates the spherical shape of the green synthesized Cv-AgNPs, which are primarily detected as individual particles with a small number observed as aggregates. Even within the aggregates, the nanoparticles were not in direct contact, indicating that a capping agent, which is naturally mono-dispersive in an aqueous environment to stabilize these particles. The synthesized silver nanoparticles lies in the size range of $10\text{--}80\text{ nm}$ according to the nanoparticle size distribution calculated with Image J software.

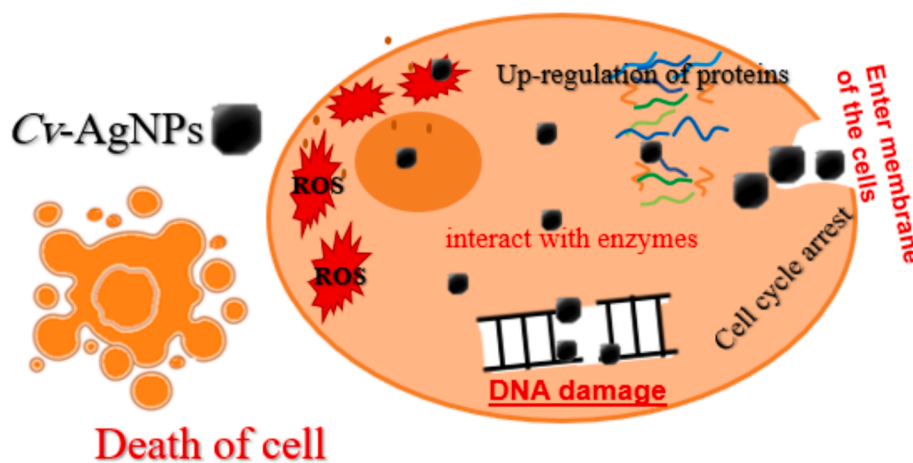
AgNP fabrication is confirmed by the high signal seen in the silver area of the EDS spectrum. Surface plasmon resonance causes metallic silver nano-crystals to typically have an optical absorption peak about 3KeV . As seen in Fig. 3C, silver was the most abundant element at 70.22% , followed by chloride (18.10%), potassium (8.79%), and zinc (1.19%). The prominent silver signal in the EDX profile confirms the reduction of silver ions to elemental silver, while the peaks for other elements may have originated from biomolecules and specific components in the CV extract (Awad et al., 2021).

To determine the average hydrodynamic size of the Cv-AgNPs, a

Table 1

Compares the efficacy of the current Cv-AgNPs with the documented potent cytotoxicity of AgNPs synthesized from various extracts reported in the literatures

| Green synthesized of AgNPs using | Cancer Types | Concentrations of AgNPs | IC50 | The viability (%) |
|---|---------------------------|-------------------------|---------------------------------------|---------------------------|
| (Khoshnevisan and Alipanah, 2022) <i>Allium sativum</i> | HepG2 | 10–40 mg/mL | 40 mg/mL | <76.17 ± 3.41 |
| (Abbas and Hussain, 2022) <i>Pomegranate leaf</i> | HeLa | 50–250 µg/mL | ≈ 100 µg/mL | ≥ 50 |
| (Sarkar and Kotteeswaran, 2018) <i>Cinnamomum verum</i> | PC-14, LC-2/ad, and HLC-1 | 1–1000 µg/mL | 259, 291, and 395 µg/mL; respectively | 20–10 |
| (Zhou and Zheng, 2022) <i>Teucrium polium</i> | NALM-6 | 1–200 µg/mL | ≈ 100–200 µg/mL | < 50(24 h) >50 (48 h) |
| (Amini and Salavati Pour, 2021) <i>Mallus domestica</i> | MCF-7 | 10–100 µg/ml | 100 µg/mL | 55 |
| (Madakka and Jayaraju, 2021) <i>Solanum macrocarpon</i> | HeLa | 10–100 µg/ml | 15.39 | 15.21 ± 0.033 |
| (Mohamed, 2024) <i>Solanum melongena</i> | MDA-MB-231 | 0–150 mg/ml | 100 mg/mL. | 50.23 |
| (Pushparaj et al., 2023) <i>Olea europaea fruit</i> | MCF-7 and T47D | 25–200 µg/mL | 143 and 77 µg/mL. | 44, and 39; respectively. |
| [current study] <i>Cinnamomum verum</i> | HeLa and MCF-7 | 1–500 µg/mL | 74.6 ± 7.43 and 55.6 ± 3.51 µg/mL | 9 % and 6 % |

**Fig. 7.** Presents a schematic depiction outlining the proposed mechanism of action of Cv-AgNPs on cancer cells.

method known as dynamic light scattering (DLS) was used in an aqueous solution. The reason for this discrepancy in size estimation could be that nanoparticles frequently occur as agglomerates, which can cause differences in the size that is observed (Ramirez-Perez et al., 2022). The synthesized nanoparticles in our study showed an average particle size distribution of 131.8 nm when assessed by intensity, according to the DLS analysis (Fig. 4A). It was determined that this distribution's intercept was 0.919. Significantly, the medium's nanoparticles showed a Polydispersity Index (PDI) of 0.160. According to reports by (Gecer et al., 2022), this PDI value indicates the monodispersity and homogeneity of the nanoparticles, implying a comparatively uniform size distribution and stability over an extended period of time. The zeta potential measurement indicated that the synthesized AgNPs have a surface charge of -22.26 mV (Fig. 4B), suggesting stability in dispersion due to specific surface charge groups. This negative charge is likely due to the adsorption of free nitrate ions, providing electrostatic stabilization (Erenler and Gecer, 2022).

The sample's crystalline nature attributes have been identified by inspected the XRD analysis. The synthesized Cv-AgNPs typical XRD patterns are displayed in Fig. 5. The high purities phase of face-centered cubic silver (COD 9011607) crystal planes may be observed with its diffraction peaks located at 2 theta 36.02° (111), 44.424° (200) and 64.95° (220) respectively. Additionally, the synthesized sample average crystallite size was calculated by using the Debye-Scherrer (Awad et al., 2021) formula and found to be 19.25 nm.

Fig. 6A and B summarizes the key data from the MTT experiment in HeLa and MCF-7 cells treated to 1 µg/ml to 500 µl for 24 h. The viability of HeLa and MCF-7 cells decreased as concentration increased. Cv-AgNPs inhibited HeLa cells 94 % and 9 % at 7.8 µl and 500 µl concentrations, respectively, and MCF-7 cells 98 % and 6 % at the same doses.

However, the maximum decrease in cells viability for both cell lines were measured as 9 % each at 500, 250, 125, 62.5 µl of Cv-AgNPs (Fig. 6 (A and B)). Cv-AgNPs significantly inhibited 50 % (IC50) of HeLa, and MCF-7 cell viability at 74.6 ± 7.43 and 55.6 ± 3.51 µg/mL; respectively. The MTT experiment also revealed a concentration-dependent reduction in the viability of HeLa and MCF-7 cells that were treated to Cv-AgNPs. The cytotoxic effects of Cv-AgNPs provide evidence that biosynthesized Cv-AgNPs could be of assistance in the quest for novel medications that can be used in chemotherapeutic treatment. The results of our study revealed that even at a concentration of 31.25 µl of Cv-AgNPs, there was a cell mortality rate over 50 %. It is possible that the cytotoxic effects generated by manufactured Cv-AgNPs at lower concentrations are caused by the plant components that are bound to the AgNPs (Dua and Giri, 2023; Genc et al., 2020; Erenler and Dag, 2022).

The cytotoxic effect of biosynthesized AgNPs has been demonstrated in numerous publications, which provides strong support for the study's findings. Upon contrasting our results with analogous investigations employing AgNPs synthesized from plant extracts documented in the literature, a number of observations became apparent. Using extracts from a variety of plants, these investigations have shown that AgNPs are capable of inhibiting the proliferation of several human cancer cell lines, including MCF-7, HeLa, and others. Furthermore, a more thorough analysis, as listed in Table 1, indicates that AgNPs derived from *Cinnamomum verum* extract consistently exhibit strong cytotoxicity and anti-proliferative activity in PC-14, LC-2/ad, and HLC-1 cell lines.

AgNPs' cytotoxic effects are explained by a generic hypothetical process that is depicted in Fig. 7. According to a number of studies, AgNPs may interact with enzymes high in thiol groups and cause partial unfolding of proteins, which would cause aggregation, once they enter cells. Additionally, presumably as a result of their disruption of protein

function, which results in modifications to cellular chemistry AgNPs also prevent human glioblastoma and cancer cells from proliferating by interfering with normal cellular processes and affecting membrane integrity, which in turn triggers apoptotic signaling pathways and cell death, according to a number of studies. Furthermore, additional studies indicate that AgNPs cause cytotoxicity by building up in the liver, where they oxidatively harm cells and encourage the production of reactive oxygen species, which triggers apoptosis (Al Baloushi, 2024; Alharbi and Felimban, 2023; Ali et al., 2022; Aziz et al., 2019).

4. Conclusion

In conclusion, silver nanoparticles (Cv-AgNPs) were successfully green-synthesized using an aqueous extract of *Cinnamomum verum*. Characterization techniques such as UV-Visible spectroscopy, FT-IR, TEM, and EDS confirmed the formation of spherical AgNPs. Also, the (FCC) crystalline structure with an average crystallite size of 19.25 nm, has been calculated by XRD patterns analysis. The biomolecules in Cv extract act as reducing and stabilizing agent, capping the core of the AgNPs. MTT assay on CMF-7 and Hela cell lines demonstrated the exceptional anticancer properties of the Cv-AgNPs, indicating their promising potential for applications in bio-nanomedicine.

Declaration of competing interest

The authors declare that they have no known competing financial interests or personal relationships that could have appeared to influence the work reported in this paper.

Acknowledgments

The authors express their gratitude to Princess Nourah bint Abdulrahman University Researchers Supporting Project number (PNURSP2024R132), Princess Nourah bint Abdulrahman University, Riyadh, Saudi Arabia.

References

- Abbas, M., Hussain, T., et al., 2022. Synthesis of silver nanoparticle from *Allium sativum* as an eco-benign agent for biological applications. *Pol. J. Environ. Stud.* 31 (1), 533–538.
- Al Baloushi, K.S.Y., et al., 2024. Green synthesis and characterization of silver nanoparticles using *Moringa peregrina* and Their Toxicity on MCF-7 and Caco-2 human cancer cells. *Int. J. Nanomed.* 3891–3905.
- Alharbi, N.S., Felimban, A.I., 2023. Cytotoxicity of silver nanoparticles green-synthesized using *Olea europaea* fruit extract on MCF7 and T47D cancer cell lines. *J. King Saud Univ.-Sci.* 35 (10), 102972.
- Ali, F., Younas, U., Nazir, A., et al., 2022. Biosynthesis and characterization of silver nanoparticles using strawberry seed extract and evaluation of their antibacterial and antioxidant activities. *J. Saudi Chem. Soc.* 26 (6), 101558.
- Amini, S.M., Salavati Pour, S., et al., 2021. Green synthesis of stable silver nanoparticles using *Teucrium polium* extract: in-vitro anticancer activity on NALM-6. *Nanomed. Res. J.* 6 (2), 170–178.
- Amirjani, A., Firouzi, F., 2020. Predicting the size of silver nanoparticles from their optical properties. *Plasmonics* 15, 1077–1082.
- Ansari, M.A., Murali, M., Prasad, D., et al., 2020. *Cinnamomum verum* bark extract mediated green synthesis of ZnO nanoparticles and their antibacterial potentiality. *Biomolecules* 10(2),336.
- Awad, M.A., Eisa, N.E., Hendi, A.A., et al., 2019. Green synthesis of gold nanoparticles: Preparation, characterization, cytotoxicity, and anti-bacterial activities. *Mater. Lett.* 256, 126608.
- Awad, M.A., Hendi, A.A., Ortashi, K.M., et al., 2021. Biogenic synthesis of silver nanoparticles using *Trigonella foenum-graecum* seed extract: Characterization, photocatalytic and antibacterial activities. *Sens. Actuators, A* 323, 112670.
- Aziz, N., Faraz, M., Sherwani, M.A., et al., 2019. Illuminating the anticancerous efficacy of a new fungal chassis for silver nanoparticle synthesis. *Front. Chem.* 7, 65.
- Das, P., Ashraf, G.J., et al., 2024. Formulation of silver nanoparticles using *Duabanga grandiflora* leaf extract and evaluation of their versatile therapeutic applications. *Bioprocess Biosyst. Eng.* 1–12.
- Demirtas, I., Erenler, R., et al., 2013. Studies on the antioxidant potential of flavones of *Allium vineale* isolated from its water-soluble fraction. *Food Chem.* 136 (1), 34–40.
- Dhaka, A., Mali, S.C., et al., 2023. A review on biological synthesis of silver nanoparticles and their potential applications. *Results in Chemistry* 101108.
- Dua, T.K., Giri, S., et al., 2023. Green synthesis of silver nanoparticles using *Eupatorium adenophorum* leaf extract: characterization, antioxidant, antibacterial and photocatalytic activities. *Chem. Pap.* 77 (6), 2947–2956.
- Easmin, S., Bhattacharyya, M., et al., 2024. Papaya peel extract-mediated green synthesis of zinc oxide nanoparticles and determination of their antioxidant, antibacterial, and photocatalytic properties. *Bioprocess Biosyst. Eng.* 47 (1), 65–74.
- Erenler, R., Dag, B., 2022. Biosynthesis of silver nanoparticles using *Origanum majorana* L. and evaluation of their antioxidant activity. *Inorganic and Nano-Metal Chemistry* 52 (4), 485–492.
- Erenler, R., Geçer, E.N., et al., 2021. Antioxidant activity of silver nanoparticles synthesized from *Tagetes erecta* L. leaves. *Int. J. Chem. Technol.* 5 (2), 141–146.
- Erenler, R., Geçer, E.N., 2022. Synthesis of silver nanoparticles using *Sideritis montana* L. leaf extract: characterization, catalytic degradation of methylene blue. *J. Nano Res.* 75, 17–28.
- Geçer, E.N., 2021. Green synthesis of silver nanoparticles from *Salvia aethiops* L. and their antioxidant activity. *J. Inorg. Organomet. Polym. Mater.* 31 (11), 4402–4409.
- Geçer, E.N., Erenler, R., Temiz, C., Genc, N., 2022. Green synthesis of silver nanoparticles from *Echinacea purpurea* (L.) Moench with antioxidant profile. *Part. Sci. Technol.* 40 (1), 50–57.
- Genc, N., Yildiz, I., Chaoui, R., et al., 2020. Biosynthesis, characterization and antioxidant activity of oleuropein-mediated silver nanoparticles. *Inorganic and Nano-Metal Chemistry* 51 (3), 411–419.
- Khan, N., Kalsoom, F., Jamila, N., Shujah, S., et al., 2023. Micromeria biflora mediated gold and silver nanoparticles for colourimetric detection of antibiotics and dyes degradation. *J. King Saud Univ.-Sci.* 35 (11), 102999.
- Khoshevisan, K., Alipanah, H., et al., 2022. Chitosan Nanoparticles Containing *Cinnamomum verum* J. Presl Essential Oil and Cinnamaldehyde; Preparation. Characterization and Anticancer Effects against Melanoma and Breast Cancer Cells. *Traditional and Integrative Medicine.*
- Madakka, M., Jayaraju, N., 2021. Evaluating the antimicrobial activity and antitumor screening of green synthesized silver nanoparticles compounds, towards MCF7 cell line (Breast cancer cell line). *Journal of Photochemistry and Photobiology* 6, 100028.
- Mani, M., Pavithra, S., Mohanraj, et al., 2021. Studies on the spectrometric analysis of metallic silver nanoparticles (Ag NPs) using *Basella alba* leaf for the antibacterial activities. *Environ. Res.* 199, 111274.
- Maruthamuthu, R., Ramanathan, K., 2016. Phytochemical analysis of bark extract of *Cinnamomum verum*: a medicinal herb used for the treatment of coronary heart disease in malayali tribes, Pachamalai Hills, Tamil Nadu, India. *International Journal of Pharmacognosy and Phytochemical Research* 8 (7), 1218–1222.
- Mohamed, M.Y.A., et al., 2024. Phyto-mediated synthesis of Ag, ZnO, and Ag/ZnO nanoparticles from leave extract of *Solanum macrocarpon*: Evaluation of their antioxidant and anticancer activities. *Inorganica Chimica Acta* 122086.
- Pradhan, S., Roy, A., Saha, A., et al., 2024. Bioinspired synthesis of silver nanoparticles using *Luffa aegyptiaca* seed extract and assessment of pharmacological properties. *Biocatal. Agric. Biotechnol.* 103209.
- Pushparaj, K., Balasubramanian, B., Kandasamy, Y., Arumugam, V.A., Kaliannan, D., Arumugam, M., et al., 2023. Green synthesis, characterization of silver nanoparticles using aqueous leaf extracts of *Solanum melongena* and in vitro evaluation of antibacterial, pesticidal and anticancer activity in human MDA-MB-231 breast cancer cell lines. *J. King Saud Univ.-Sci.* 35 (5), 102663.
- Ramirez-Perez, J.C., Reis, T.A., et al., 2022. Impact of silver nanoparticles size on SERS for detection and identification of filamentous fungi. *Spectrochim. Acta Part A: Mol. Biomol. Spectrosc.* 272, 120980.
- Rizki, I.N., Inoue, T., Chuaicham, C., et al., 2023. Fabrication of Reduced Ag nanoparticle using crude extract of cinnamon decorated on ZnO as a photocatalyst for hexavalent chromium reduction. *Catalysts* 13, no. 2, 265. <https://doi.org/10.3390/catal13020265>.
- Saqib, S., Faryad, S., Afridi, M.I., et al., 2022. Bimetallic assembled silver nanoparticles impregnated in *Aspergillus fumigatus* extract damage the bacterial membrane surface and release cellular contents. *Coatings* 12 (10), 1505.
- Sari, Y.P., Suchi, A.Q., 2023. Biosynthesis and Characterization of Silver Nanoparticles using Single Garlic Callus Extract (*Allium sativum* L.). *Malaysian J. Fundam. Appl. Sci.* 19 (4), 563–572.
- Sarkar, S., Kotteeswaran, V., 2018. Green synthesis of silver nanoparticles from aqueous leaf extract of Pomegranate (*Punica granatum*) and their anticancer activity on human cervical cancer cells. *Adv. Nat. Sci. Nanosci. Nanotechnol.* 9 (2), 025014.
- Sharma, V., Verma, D., Okram, G.S., 2020. Influence of surfactant, particle size and dispersion medium on surface plasmon resonance of silver nanoparticles. *J. Phys. Condens. Matter* 32 (14), 145302.
- Vikulova, E.S., Karakovskaya, K.I., et al., 2023. Application of biocompatible noble metal film materials to medical implants: TiNi surface modification. *Coatings* 13 (2), 222.
- Zhou, J., Zheng, X., et al., 2022. Introducing a Novel Chemotherapeutic Drug for the Treatment of Lung Adenocarcinoma: Silver Nanoparticles Green-formulated by *Cinnamomum verum*. *J. Oleo Sci.* 71 (3), 371–378.
- Zia, M., Gul, S., Akhtar, J., Haq, I.U., et al., 2017. Green synthesis of silver nanoparticles from grape and tomato juices and evaluation of biological activities. *IET Nanobiotechnology* 11 (2), 193–199.